Step dynamics in faceting on vicinal Si(113) surfaces

2003 J. Phys.: Condens. Matter 15 S3241

(http://iopscience.iop.org/0953-8984/15/47/004)

INSTITUTE OF PHYSICS PUBLISHING JOURNAL OF PHYSICS: CONDENSED MATTER

J. Phys.: Condens. Matter **15** (2003) S3241–S3253 PII: S0953-8984(03)67198-5

Step dynamics in faceting on vicinal Si(113) surfaces

K Sudoh and H Iwasaki

The Institute of Scientific and Industrial Research, Osaka University, 8-1 Mihogaoka, Ibaraki, Osaka 567-0047, Japan

Received 5 August 2003
Published 14 November 2003
Online at stacks.iop.org/JPhysCM/15/S3241

Abstract

Faceting is a thermodynamic phase separation where a surface with some arbitrary macroscopic orientation breaks up into a hill and valley structure. Vicinal Si(113) surfaces are typical systems where faceting occurs due to short-range attractive step–step interactions. This paper reviews our recent studies on step dynamics involved in faceting on vicinal Si(113) surfaces, by high temperature scanning tunnelling microscopy and analysis based on the continuum step model.

1. Introduction

Faceting is a first-order orientational phase transition induced by anisotropy in surface free energy. Below the transition temperature, the surface spontaneously rearranges into a hill and valley structure composed of facets with two or more orientations. Various physical situations cause faceting; for example, chemical adsorption [1, 2], surface reconstructions [3–6] and attractive interactions between atomic steps [7, 8].

Though the thermodynamic theory for faceting has long been well established [9–11], the kinetics of faceting presents a long-standing problem for surface physics. Mullins [2] pioneered the study of the kinetics of facet growth, developing a one-dimensional mathematical formulation in terms of a continuum surface model. However, for a detailed and quantitative understanding of faceting dynamics, exploration of the involved step dynamics is necessary, since the surface mass transport depends on the nature of the steps below the roughening temperature [13]. In addition to theoretical efforts to understand the facet growth by a step model [14–16], recent advances in real-time surface monitoring techniques, such as low energy electron microscopy (LEEM) and scanning tunnelling microscopy (STM), make it possible to perform experimental investigations in terms of the step dynamics, allowing significant insights into faceting dynamics.

With Si surfaces, two distinct cases have been observed experimentally for the reversible phase transformation between the high temperature stepped phase and the low temperature faceted phase. One is the faceting on Si(111) surfaces observed by LEEM [3, 4] and STM [17, 18], where faceting is induced by the stability of the 7×7 surface reconstruction that causes nucleation and subsequent growth of terraces with the 7×7 reconstruction, pushing

0953-8984/03/473241+13$30.00

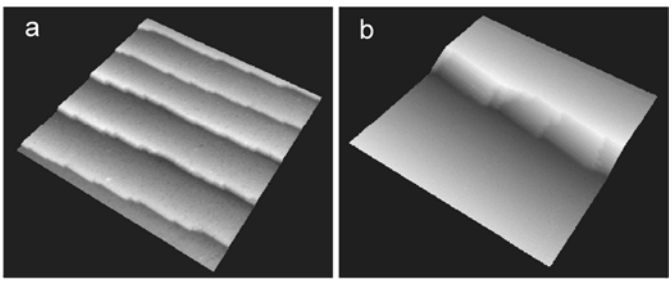

Figure 1. 130 nm × 130 nm STM images showing a faceting transition on the Si(113) surface miscut towards [$\bar{3}\bar{3}2$]. The samples were annealed at (a) 750 °C and (b) 1100 °C.

adjacent steps into a second, high step density, phase. The alternative case is the faceting on Si(113) surfaces discovered by Song and co-workers using surface x-ray scattering [7, 8]. Recent statistical mechanics studies have shown that the observed orientational phase diagram for Si(113) vicinal surfaces is characteristic of surfaces with short-range attractive step–step interactions and long-range repulsive step–step interactions [19–23].

Though the kinetics of facet growth via facet nucleation originally predicted by Mullins, which is accepted as the mechanism for experimentally observed faceting induced by the surface reconstruction and adsorption on various surfaces, is now well understood, the dynamics of faceting induced by attractive step–step interactions is less investigated and many open issues exist. In this paper we review the advances in understanding the dynamics of faceting driven by attractive step–step interactions from our recent experimental investigations of faceting on Si(113) surfaces, and from analysis based on the continuum step model. This paper is organized as follows. In section 2, we briefly explain the microscopic structure of faceted Si(113) surfaces and present an argument for the origin of the attractive step–step interactions. Section 3 describes the time dependence of the average terrace width during faceting on Si(113) surfaces. In section 4, results of real-time observation of surface evolution during faceting on Si(113) surfaces by high temperature STM are given. Section 5 discusses the mechanism of zipping up the neighbouring steps, which is the most dominant process for faceting on Si(113) surfaces, based on the continuum step model. In section 6, we describe a simulation using the step network model that has been constructed as a kinetic model for coarsening of a step network. We demonstrate that this model can well reproduce the experimental results.

In the experiment, two kinds of Si(113) substrates were used. One is a Si(113) surface miscut by 1° towards the direction of high symmetry and the other is a Si(113) surface miscut by 1.7° along a low symmetry azimuth, which is rotated 57° from [$\bar{3}\bar{3}2$] to [$\bar{1}10$]. The experiments were conducted in a ultrahigh vacuum chamber equipped with a variable temperature STM (JSTM-4610 from JEOL).

2. Structure formed on vicinal Si(113) surfaces

Before we discuss faceting dynamics, we briefly set out the structure formed on Si(113) surfaces and present an argument for the origin of the attractive step–step interaction. Figure 1 shows STM images of a Si(113) surface miscut along [$\bar{3}\bar{3}2$] annealed at 750 and 1100 °C, which are, respectively, below and above the faceting transition temperature of 950 °C for this sample [7, 8] and which clearly illustrates the faceting transition. These STM images were obtained at room temperature after quenching the samples. While annealing above the

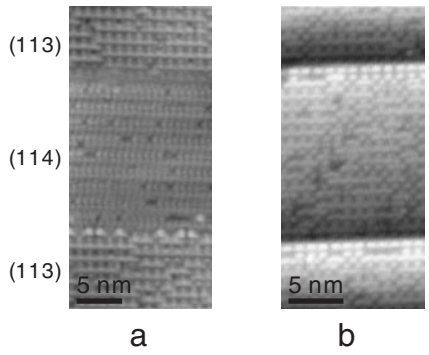

Figure 2. High resolution STM images of Si(113) surfaces miscut towards $[\bar{3}\bar{3}2]$. (a) A surface composed of (113) facets and (114) facets. (b) A surface with double steps.

transition temperature leads to a uniformly stepped structure, annealing below the transition temperature causes a break-up of the surface into a hill and valley structure composed of (113) facets and (114) facets. High resolution STM images of a Si(113) surface are shown in figure 2. Figure 2(a) shows an STM image of a faceted structure composed of 3×2-reconstructed (113) facets [24, 25] and a 2×1-reconstructed (114) facet [26, 27]. The (114) facet found in this image corresponds to a bunch of ten single steps. (The height of a single step is 1.64 Å.) The smallest size of a (114) facet we observed was four layers high. Moreover, double steps with a well defined atomic structure different from those on the (114) facet are also stable (figure 2(b)). On Si(113), the 3×2 reconstructed surface is most stable at room temperature and experiences a phase transition to the 3×1 reconstructed phase at about 500 °C [28, 29]. It is known that the 3×1 reconstruction disorders continuously in a second-order transition at about 700 °C [28–33]. Because the faceting transition temperature is much higher than this order–disorder transition temperature, the reconstructions on the Si(113) facet do not relate to the faceting transition. Thus we consider that faceting on Si(113) is induced by the increased stability of the bunched steps, which is most likely due to local rebonding at the step edges. We can regard the stabilization of such bunched states as the result of a reduction of the surface free energy due to the short-range attractive interactions between single steps, since rebonding occurs for steps separated by the specific short distance. A rough estimation of the attractive interaction energy will be presented in section 5.

On the Si(113) surfaces miscut along a low symmetry azimuth, though the faceting temperature is much lower than that of the Si(113) surfaces miscut towards $[\bar{3}\bar{3}2]$, faceting occurs [34, 35]. Despite the low symmetry surface orientation, the morphology of the faceted surfaces is uniaxial. Figure 3 shows a high resolution STM image of the structure of a step bunch of five-layer height on the Si(113) surface miscut along the azimuth, which is 57° away from $[\bar{3}\bar{3}2]$. The faceting temperature of this surface is 720 °C [34]. On this low symmetry surface, no well-defined facets such as the (114) facets are formed and the structure of the step bunch is quite different from that on the surfaces miscut along $[\bar{3}\bar{3}2]$. The slope of the step bunch is in the range of 7°–18°, which is much larger than that of the (114) facet, i.e. 5.7°. At the edge of the step bunch, atomically rough structures due to splitting of the step bunch into single and double steps with zigzag structures are observed. Though long-range ordering does not arise, local rebonding stabilizes the bunched steps even on such a low symmetry surface. The lowered faceting temperature on the surface miscut along a low symmetry azimuth is most likely to be caused by decreased stability due to the atomically disordered structure of the step bunches.

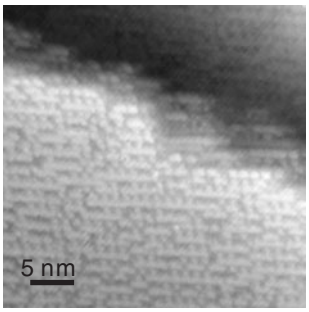

Figure 3. A high resolution STM image of the step bunch of five-layer height on the Si(113) surface miscut along the direction which is 57° away from $[\bar{3}\bar{3}2]$.

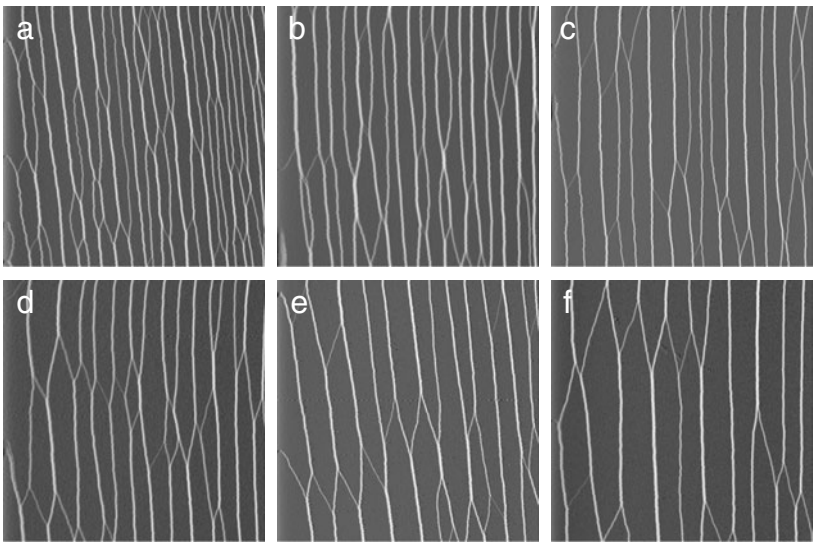

Figure 4. 1300 nm × 1300 nm STM images of Si(113) surfaces miscut along the direction which is 57° away from $[\bar{3}\bar{3}2]$. The images were taken at room temperature after annealing at 600 °C for (a) 1 min, (b) 4 min, (c) 8 min, (d) 16 min, (e) 32 min and (f) 64 min.

3. Time dependence of terrace width

A rapid temperature decrease through the faceting temperature initiates a break-up of the surface into a hill and valley structure. In the subsequent surface evolution, the morphology gradually coarsens under a far-from-equilibrium condition. We have experimentally investigated the morphological changes during the surface coarsening process driven by the attractive step–step interactions on a Si(113) surface miscut by 1.7° along the direction which is 57° away from $[\bar{3}\bar{3}2]$ [34]. Figure 4 shows STM images of Si(113) surfaces annealed at 600 °C for various times after being quenched from 1000 °C within a few seconds. On the surfaces, step bunches with various sizes coexist. The step bunches sporadically fork, forming a two-dimensional network of step bunches. As annealing time increases, the network structure gradually coarsens with increasing sizes of the step bunches. To quantitatively characterize the surface coarsening, we have measured the characteristic length scale L for the structure as a function of annealing time from STM images such as those shown in figure 4. Figure 5

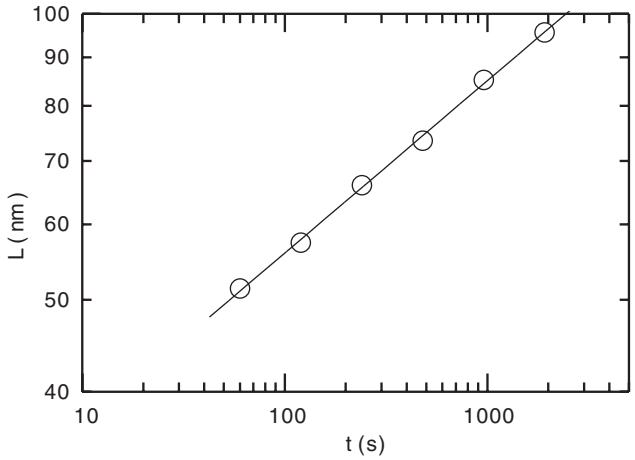

Figure 5. A log–log plot of the average terrace width measured from STM images as a function of annealing time for an annealing temperature of 600 °C. The plot shows that the average terrace width has a power law dependence on the annealing time. The exponent is estimated to be 0.18 ± 0.02.

shows a log–log plot of the measured average terrace width versus the annealing time for annealing temperatures of 600 °C, showing a power law dependence, i.e. $L(t) \sim t^{\phi}$. From the data, the exponent ϕ is determined to be 0.18 ± 0.02, which is consistent with the time scaling, $t^{1/6}$. This dynamic scaling property was also obtained on the Si(113) surface miscut towards $[\bar{3}\bar{3}2]$ by Song and co-workers using x-ray scattering measurements [36, 37]. The obtained time dependence of an average terrace width as $t^{1/6}$ is quite different from the time evolution as $t^{1/4}$ expected for faceting via nucleation [1, 12]. This discrepancy arises because the driving force for faceting on Si(113) is short-range attractive step–step interactions. We will show that the scaling exponent of approximately $1/6$ is characteristic for coarsening of a step–bunch network driven by short-range attractive step–step interactions, performing a numerical simulation based on the continuum step model, in section 6.

4. Real-time observation of step dynamics during faceting

We have observed in real time how a network of step bunches coarsens during faceting by high temperature STM; the dominant mechanism for coarsening of a step–bunch network was revealed [38, 39]. Unfortunately the process by which a network of step bunches are formed from a uniformly stepped surface in the very early stage of faceting cannot be observed by STM, since we have to wait at least 10 min before observation due to the thermal drifting of samples.

Figure 6 shows a sequence of STM images of the Si(113) surface miscut by 1.0° toward $[\bar{3}\bar{3}2]$ during annealing at 600 °C [34]. On this high symmetry surface, an array of straight step bunches along the $[\bar{1}10]$ direction is formed, and the density of defect structures, i.e. step–bunch junctions, is relatively low. The image in figure 6(a) was observed 23 min after quenching the sample to 600 from 1000 °C. At such late times, step bunches of relatively large sizes have already been formed and step bunches of from 3 to 10 layers in height coexist. These step bunches are noticeably stable and hardly move. Distinct structural changes can be seen around the defect structures in the array of step bunches. As indicated by arrows in figure 6, the ramified structures propagate along the step direction, just like 'zipping up', forming larger step bunches.

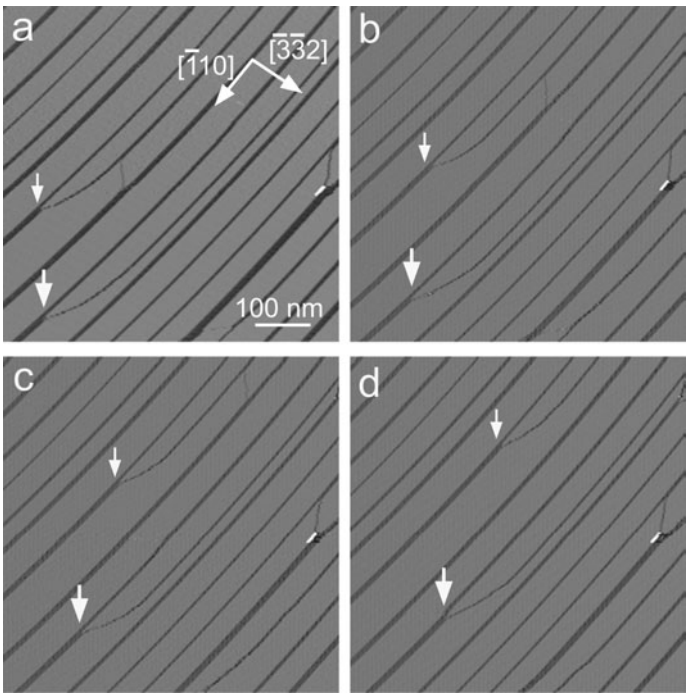

Figure 6. A series of STM images showing the evolution of surface morphology during faceting on the Si(113) surface miscut towards [$\bar{3}\bar{3}$2]. The images are obtained after quenching the surface to 600 °C: (a) 1390 s, (b) 1610 s, (c) 1900 s and (d) 2300 s. Two examples of zipping are indicated by small and large arrows. A pinning site, which appears as a bright structure at the centre right in all images, serves as a marker for measuring quantitatively step displacements between sequential images.

When a fine network of step bunches is formed, as shown in figure 4, the features of the structural changes during faceting are more complicated. The sequence of STM images shown in figure 7 manifests how a step bunch network coarsens via step motion. This result was obtained, during annealing at 600 °C, on a Si(113) sample miscut along the low symmetry azimuth. In this example, distinct changes in the step configuration are recognized only in the vicinity of points where two step bunches merge and zipping moves are dominant for surface evolution. Another characteristic feature is that the zipping move leads to changes in the topological configuration of the network. For example, as indicated by the small arrow in figure 7, the neighbouring step bunches are mediated to approach each other by a crossing step trapped between them and are finally bound, which causes a change in the local topological configuration. In figure 8, the measured distance l between the step bunches which are connected by a crossing step as a function of time is shown. When the distance between the step bunches decreases down to $\sim$30 nm, the step bunches suddenly contact each other and the H-shaped configuration varies into an X-shaped one. Though the mechanism of this behaviour has not been investigated in detail, the onset of this topological change is associated with thermal fluctuations of the step bunches since this kind of change in step–bunch topology was not observed at somewhat lower temperatures. From the overall results obtained by real-time STM observation, we concluded that, during faceting, structural change is irreversible and a fine network of step bunches formed in the very early stage, coarsens via zipping up of the neighbouring step bunches and alteration of the network topology.

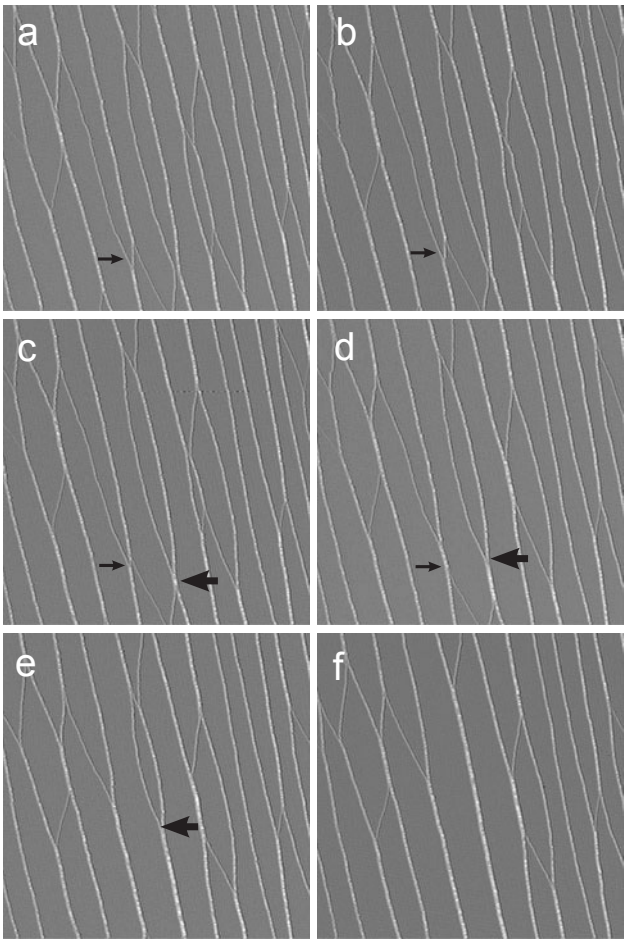

Figure 7. The time evolution of surface morphology during faceting on the Si(113) surface miscut along the direction which is 57° away from $[\bar{3}\bar{3}2]$ at 600 °C. The images correspond to (a) 530 s, (b) 610 s, (c) 650 s, (d) 690 s, (e) 930 s and (f) 1085 s, after starting to anneal at 600 °C.

5. Mechanism of zipping move

The basic theory of the motion of continuous steps was well established for various physical situations [13, 14, 40]. The observed zipping motion can be understood in terms of the continuum step model. Here, the position of the step is denoted by $x(y)$, where the y direction is take to be the step direction (figure 9). Assuming attachment/detachment limited kinetics, the equation for the motion of a n-layer high step is given by

$$\frac{\partial x}{\partial t} = \frac{\Gamma_n \beta_n}{kT} \frac{\partial^2 x}{\partial y^2}, \tag{1}$$

where β_n is the step tension (or the step stiffness) and Γ_n is the mobility of the step. The dynamic behaviour of a ramified structure where a step bunch merges into the adjacent straight step bunch, as schematically shown in figure 9, can be analysed based on this equation. Here we assume that a step bunch always contacts with the neighbouring step bunch at an angle that minimizes the local surface free energy [41]. Under a boundary condition $x(y_i, t) = 0$,

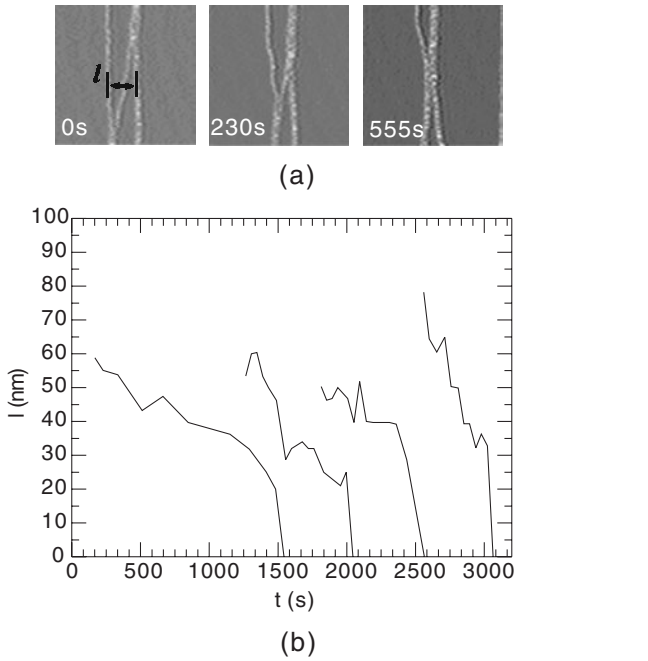

Figure 8. (a) An example of crossing-step-mediated approaching of step bunches that leads to a change in the network topology locally. (b) The time dependence of the distance l between the step bunches. When the distance l decreases down to about 30 nm, the two step bunches suddenly contact each other.

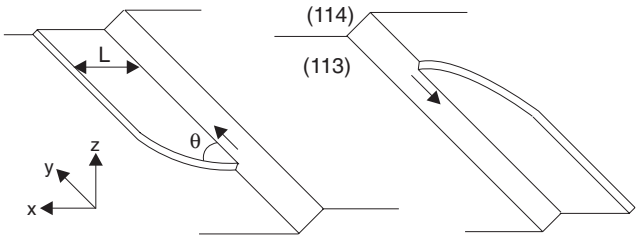

Figure 9. Schematic picture of zipping up of the neighbouring step bunches.

$x(y \to \infty, t) = L$ and $x'(y_i, t) = \tan\theta$, where y_i is the position at which the step bunches intersect each other, we obtain a shape preserving solution:

$$x(y,t) = L - L\exp\left\{-\frac{\tan\theta}{L}y + \frac{\Gamma_n\beta_n\tan^2\theta}{kTL^2}t\right\}. \tag{2}$$

This solution implies that a stable step profile:

$$f(y) = L - L\exp\left(-\frac{\tan\theta}{L}y\right), \tag{3}$$

propagates along the y direction with a constant velocity:

$$v = \frac{\Gamma_n\beta_n\tan\theta}{kTL}. \tag{4}$$

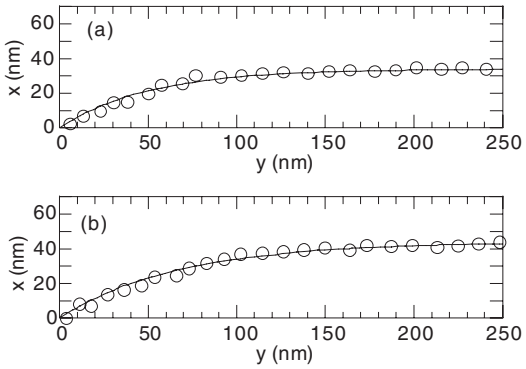

Figure 10. Positions of the step edges measured on the STM images are plotted with open circles. Panels (a) and (b) are the data for the steps indicated by small and large arrows in figure 6. The full curves are the step shape calculated by equation (3), using the parameters estimated from the STM data: (a) $L = 34$ nm, $\theta = 35°$; (b) $L = 44$ nm, $\theta = 33°$.

This result suggests that the areal rate of zipping, vL, is a constant dependent only on the attachment/detachment rate, the step tension and the attractive interaction energy (which is introduced through the value of θ).

The above theoretical prediction can be directly compared with the STM observations shown in figure 6 where two sample structures with $L = 34$ and 44 nm appear. In figure 10, the profiles for these four-layer high steps are plotted with the step shape predicted from equation (3), showing good agreement with theory. For these steps, the measured speeds of step motion during zipping are 0.30 ± 0.02 and 0.24 ± 0.02 nm s^{-1}, respectively. Thus we can confirm that vL is a constant and the value of $\Gamma_4\beta_4/kT$ is estimated to be 15 ± 3 nm^2 s^{-1}.

In the above argument in respect to zipping motions, the effect of the attractive step–step interaction is introduced through the equilibrium contact angle θ. By measuring θ, the attractive step–step interaction can be estimated. The equilibrium contact angle, which minimizes the local surface free energy, will be determined by a competition between the energy gained from the attractive interaction in forming the larger step bunch, and the energy lost from increasing the length of the step edge [41]. The equilibrium contact angle θ is given by

$$\cos\theta = \frac{nh}{\beta_n \tan\phi}\left(\frac{\gamma_{\text{bunch}}}{\cos\phi} - \gamma_{113}\right), \tag{5}$$

where γ_{bunch} and γ_{113} are the surface free energy per unit area of step bunches and (113) facets, ϕ is the angle between the (113) facet and the step bunch and h is the height of single steps. Assuming that the repulsive interaction between steps is negligible, the surface free energy of step bunches (i.e. (114) facets) can be expressed as $\gamma_{\text{bunch}}/\cos\phi = \gamma_{113} + (\tan\phi/h)\beta_1 - E_{\text{b}}$, where E_{b} is the stabilization energy (per projected area in the (113) plane) for the step bunches. Using equation (5), the stabilization energy can be expressed as $E_{\text{b}} = (\tan\phi/nh)(n\beta_1 - \beta_n\cos\theta)$, and thus the energy gain per unit length for forming a 114-orientated step bunch of n-layers height is given by $n\beta_1 - \beta_n\cos\theta$. Assuming that the binding energy scales linearly with the step height, the attractive interaction between neighbouring single-layer height steps is given by

$$E_{\text{a}} = \frac{n\beta_1 - \beta_n\cos\theta}{n-1}. \tag{6}$$

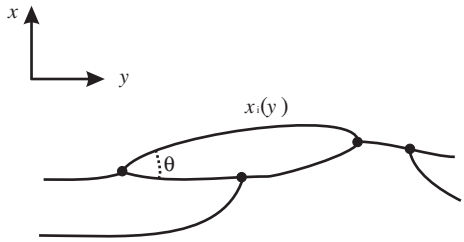

Figure 11. Schematic picture of the step network model.

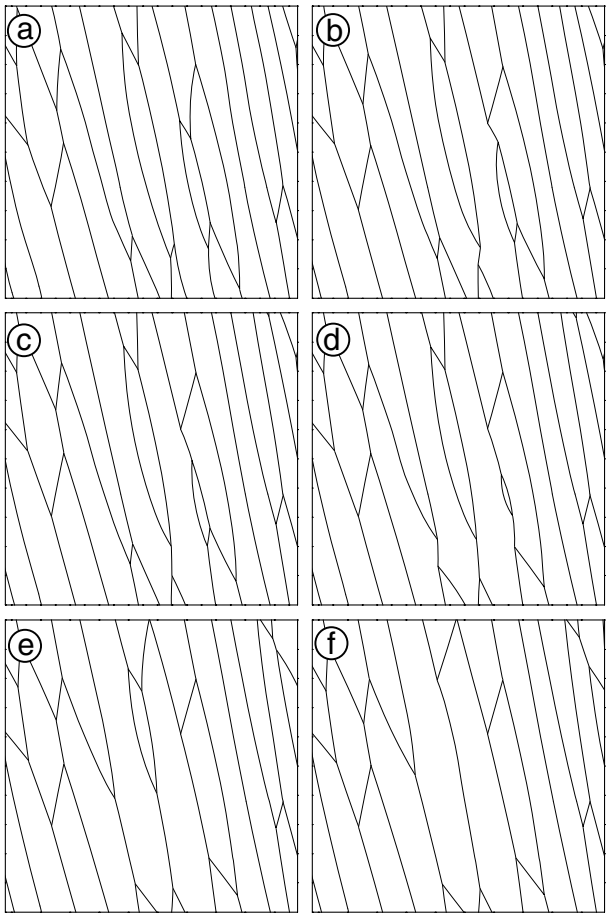

Figure 12. Sequence of configurations generated in the simulation of the step network model. (a) Starting configuration created from the experimental data in figure 7(a). The configurations correspond to (b) $\tau = 7000$, (c) $\tau = 11\,000$, (d) $\tau = 14\,000$, (e) $\tau = 36\,000$, and (f) $\tau = 50\,000$, where τ is the rescaled time and $t(\Gamma_1\beta_1/kT)$.

Using $\phi = 5.7°$, $h = 1.64$ Å, $\beta_4 = 220$ meV Å^{-1} and $\beta_1 = 57$ meV Å^{-1} which were previously obtained at 710 °C [42], we can estimate the binding energy for a single-layer high step to be roughly 15 meV Å^{-1} from equation (6).

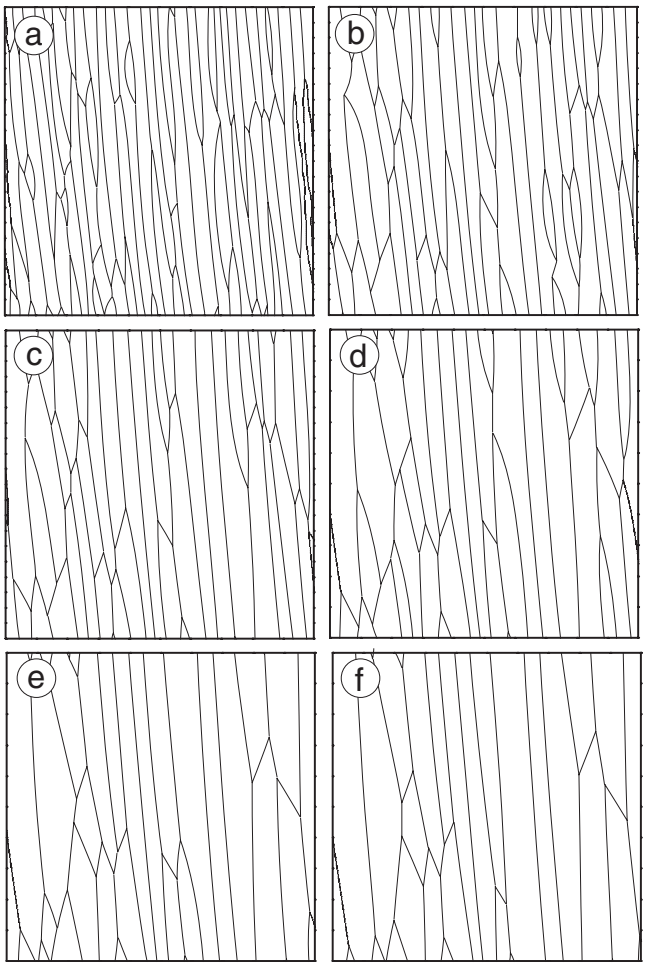

Figure 13. Sequence of configurations generated by the simulation.

6. Step network model

We extended the continuum step model to a study of the two-dimensional pattern evolution of a step network and demonstrated that the step network model reproduces not only the time scaling behaviour but also real-time evolution of surface morphology on a Si(113) surface [39]. The surface morphology is represented by a network of strings where each string is connected with two other strings at both ends, as schematically shown in figure 11. The time evolution of each step via a zipping motion can be described by equation (1) with the boundary condition at the junction of the steps. We assume that a step bunch always contacts with the neighbouring step bunches at the equilibrium angle θ given by equation (5). In general, both the mobility and the tension of the step bunch appearing in equations (1) and (5) depend on the bunch size n. We assume here that $\beta_n = n\beta_1$ and $\Gamma_n = \Gamma_1/n$; therefore the factor of n cancels in equations (1) and (5) and the behaviour of each step bunch is independent of its bunch size. Previously we confirmed the linear dependence of the step stiffness on bunch size using STM [42]. Yamamoto [43] predicted these dependences of the stiffness and the mobility for a group of steps on rough surfaces.

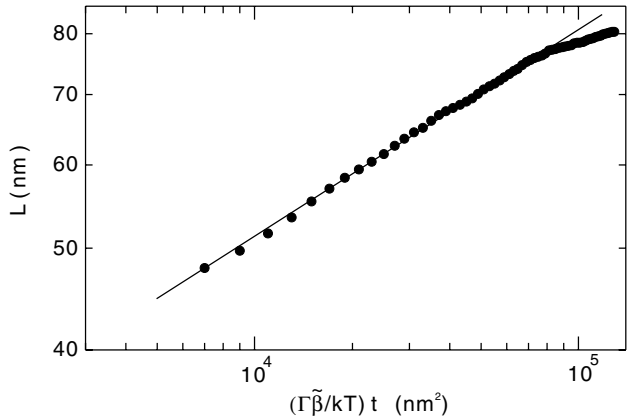

Figure 14. The time evolution of the average terrace width obtained by the simulation for $l_c = 35$ nm and $\theta = 30°$.

As observed in figure 7, a zipping motion leads to a change in topological configuration of the step network when the distance between junctions becomes sufficiently small. In particular, the reconnection in the network configuration from a H-shaped connection with a crossing step to a X-shaped connection, as shown in figure 8, plays an important role in the coarsening of the network since it triggers another zipping move. The model described above, since it contains no term representing a strong bunch–bunch interaction, cannot describe this type of topological change. To incorporate such irreversible binding events that lead to step–bunch merging, during relaxation of a step network, we mechanically change the topological configuration, introducing a characteristic length l_c as an empirical parameter. Numerically integrating equation (1) while allowing the alteration of the topological configuration of the network, allows for large-scale simulation of coarsening of a step network to be performed.

Figure 12 indicates the results of the numerical simulation where the step configuration extracted from the STM image in figure 7(a) is used as an initial configuration, showing good agreement with the experimentally observed time evolution (figure 7). In this simulation, parameters estimated from the experimental results, $\theta = 30°$ and $l_c = 35$ nm, are used. From comparison between the timescales in the simulation and the experiment, $\Gamma_1\beta_1/kT$ is estimated to be 90 ± 20 nm^2 s^{-1}.

To quantify the scaling property in the kinetic step network model, we performed larger scale simulations, using the step configuration extracted from the 1300 nm $\times$ 1300 nm STM images of a surface quenched from 1000 °C to room temperature as initial configurations. On each of the initial surfaces, a fine random network composed of mainly single, double and triple steps is formed. Figure 13 shows an example of the simulation results. The calculated time dependence of average terrace widths is shown in figure 14. This result is averaged over nine individual calculations with different initial configurations. The obtained time dependence of the average terrace width is consistent with the power law dependence on time, though the range of the data is too narrow because of the simulation in a finite system size. The obtained exponent is 0.18 ± 0.02, which is consistent with time dependence as $t^{1/6}$.

7. Conclusions

In this paper, we reviewed our recent studies on far-from-equilibrium dynamics of faceting on Si(113) surfaces induced by short-range attractive step–step interactions. The distinct step

dynamics involved in faceting have been revealed by real-time STM imaging of the surface evolution. During faceting, the two-dimensional network of step bunches, formed in the initial stage of faceting, coarsens via zipping and alteration of the network topology. The continuum step model yields a quantitative understanding of the observed zipping of the neighbouring step bunches. Based on STM observation, we have constructed a step network model that enables us to simulate the surface evolution occurring during faceting driven by attractive step–step interactions.

Acknowledgment

We are grateful to Professor E D Williams for the fruitful collaboration.

References

[1] Ozcomert J S, Pai W W, Bartelt N C and Reutt-Robey J E 1994 *Phys. Rev. Lett.* **72** 258
[2] Ozcomert J S, Pai W W, Bartelt N C and Reutt-Robey J E 1994 *J. Vac. Sci. Technol.* A **12** 2224
[3] Phaneuf R J, Bartelt N C and Williams E D 1991 *Phys. Rev. Lett.* **67** 2986
[4] Phaneuf R J, Bartelt N C, Williams E D, Swiech W and Bauer E 1993 *Phys. Rev. Lett.* **71** 2284
[5] Watson G M, Gibbs D, Zehner D M, Yoon M and Mochrie S G J 1993 *Phys. Rev. Lett.* **71** 3166
[6] Watson G M, Gibbs D, Zehner D M, Yoon M and Mochrie S G J 1998 *Surf. Sci.* **407** 59
[7] Song S and Mochrie S G J 1994 *Phys. Rev. Lett.* **76** 4568
[8] Song S and Mochrie S G J 1995 *Phys. Rev.* B **51** 10068
[9] Herring C 1951 *Phys. Rev.* **82** 87
[10] Nozieres P 1991 *Solids Far from Equilibrium* (Cambridge: Cambridge University Press)
[11] Williams E D 1994 *Surf. Sci.* **299/300** 502
[12] Mullins W W 1961 *Phil. Mag.* **6** 1313
[13] Jeong H C and Williams E D 1999 *Surf. Sci. Rep.* **34** 171
[14] Liu D J, Weeks J D, Johnson M D and Williams E D 1997 *Phys. Rev.* B **55** 7653
[15] Jeong H C and Weeks J D 1995 *Phys. Rev. Lett.* **75** 4456
[16] Jeong H C and Weeks J D 1998 *Phys. Rev.* B **57** 3949
[17] Hibino H, Homma Y and Ogino T 1995 *Phys. Rev.* B **51** 7753
[18] Suzuki M *et al* 1993 *J. Vac. Sci. Technol.* A **11** 1640
[19] Bhattacharjee S M 1996 *Phys. Rev. Lett.* **76** 4568
[20] Bhattacharjee S M and Mukherji S 1999 *Phys. Rev. Lett.* **83** 2374
[21] Lässig M 1996 *Phys. Rev. Lett.* **77** 526
[22] Shenoy V B, Zhang S and Saam W F 1998 *Phys. Rev. Lett.* **81** 3475
[23] Shenoy V B, Zhang S and Saam W F 2000 *Phys. Rev.* B **467** 58
[24] Knall J, Pethica J B, Todd J D and Wilson J H 1991 *Phys. Rev. Lett.* **66** 1733
[25] Dąbrowski J, Müssig H J and Wolff G 1995 *Surf. Sci.* **331–333** 1022
[26] Erwin S C, Baski A A and Whitman L J 1996 *Phys. Rev. Lett.* **77** 687
[27] Baski A A, Erwin S C and Whitman L J 1997 *Surf. Sci.* **392** 69
[28] Schreiner J, Jacobi K and Selke W 1994 *Phys. Rev.* B **49** 2706
[29] Hibino H and Ogino T 1997 *Phys. Rev.* B **56** 4092
[30] Olshanetsky B Z and Mashanov V I 1981 *Surf. Sci.* **111** 414
[31] Yang Y N, Williams E D, Park R L, Bartelt N C and Einstein T L 1990 *Phys. Rev. Lett.* **64** 2410
[32] Abernathy D L, Birgeneau R J, Blum K I and Mochrie S G J 1993 *Phys. Rev. Lett.* **71** 750
[33] Abernathy D L, Song S, Blum K I, Birgeneau R J and Mochrie S G J 1994 *Phys. Rev.* B **49** 2691
[34] Sudoh K, Yoshinobu T and Iwasaki H 1998 *Japan. J. Appl. Phys.* **37** 5870
[35] Yoon M, Mochrie S G J, Tate M W, Gruner S M and Eikenberry E F 1998 *Surf. Sci.* **411** 70
[36] Song S, Mochrie S G J and Stephenson G B 1995 *Phys. Rev. Lett.* **74** 5240
[37] Song S, Yoon M, Mochrie S G J, Stephenson G B and Milner S T 1997 *Surf. Sci.* **372** 37
[38] Sudoh K, Iwasaki H and Williams E D 2000 *Surf. Sci.* **452** L287
[39] Sudoh K and Iwasaki H 2001 *Phys. Rev. Lett.* **87** 216103
[40] Bartelt N C, Goldberg J L, Einstein T L and Williams E D 1992 *Surf. Sci.* **273** 252
[41] Li B, Bartelt N C and Williams E D 1994 *Chem. Phys. Lett.* **217** 595
[42] Sudoh K, Yoshinobu T, Iwasaki H and Williams E D 1998 *Phys. Rev. Lett.* **80** 5152
[43] Yamamoto T 2001 unpublished